Chapter 1

Introduction

1.1 Introduction

During the last two decades, hydrogenated nanocrystalline silicon (nc-Si:H) thin films have triggered great interest in research on the growth, characterization and application of this material. This material has attracted considerable attention due to their potential applications in optoelectronic devices such as single electron transistors, solar cells and thin film transistors (TFTs). This interest on nc-Si:H research is reflected by the number of publications in journals and conferences over the two decades as obtained from SciFinder shown in Figure 1.1. Mixed phased nc-Si:H material consisting of Si nano-crystallites embedded within an amorphous matrix has better optical, structural and electrical properties compared to hydrogenated amorphous silicon (a-Si:H) thin films. However, research on silicon nanostructures which cover Si quantum dots and wires nanostructures have also gained almost similar attention over these years and is expected to gain increased attention due to their unique properties as a result of the high surface to volume ratio of the material.

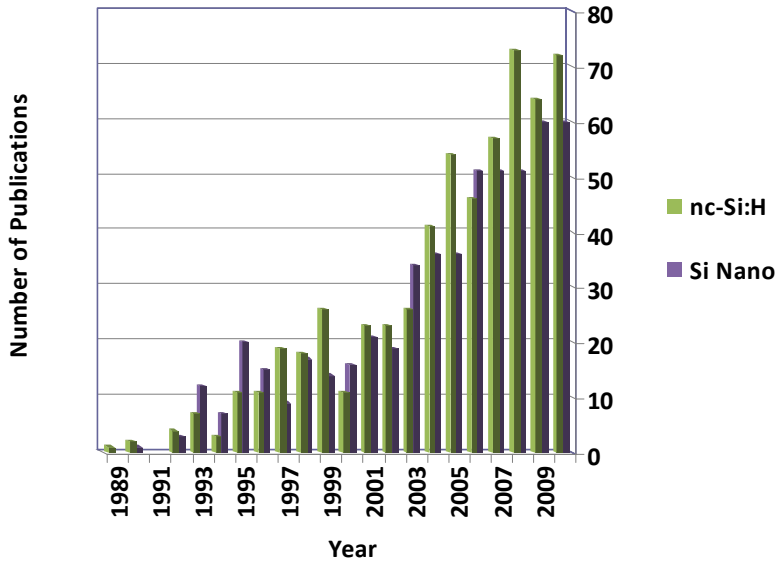

Figure 1.1: Distribution of hydrogenated nanocrystalline silicon (nc-Si:H) and silicon nanostructure publications in journals and conference presentations as obtained from SciFinder.

1.2 Evolution from Amorphous Silicon to Nanocrystalline Silicon

Amorphous silicon (a-Si) made its emergence in the early 1960s and deposition was mainly through sputtering a silicon target or by thermal evaporation resulting in material with high defect density. Sterling & Swann, were the first to use PECVD to grow a-Si:H along with silicon oxide (SiO) and amorphous silicon nitride (a-SiN:H) using silane (SiH_4) gas as the main precursor gas in 1965. The use of SiH_4 gas resulted in hydrogen incorporation into the film structure and this film since then has been referred to as hydrogenated amorphous silicon (a-Si:H). The hydrogen passivation of dangling bond in the films reduced defects in the film structure and made doping of the films possible. This created immense interest on the material for potential electronic applications then. However, the low performance of a-Si:H in device applications compared to crystal silicon made it less popular as an electronic material but vast interest amongst researchers on this material makes research on this material even relevant until today.

In 1968 Veprek and Marcek first synthesized hydrogenated microcrystalline silicon (μc-Si:H), which showed much more superior properties as an electronic material at low temperature using a remote PECVD system. Later, in 1981 Spear joined Veprek to synthesize μc-Si:H from SiH_4 highly diluted in hydrogen by pulsed PECVD. Research was focused on the optical properties (Richter & Ley, 1981), microstructure studies (Nagata *et al.*, 1981, Iqbal & Veprek, 1982) and electrical properties (Willeke *et al.*, 1982). Next research on potential applications of μc-Si:H in solar cells became the focus of interest starting with the growth of highly doped *n*-type μc-Si:H layer by Moustakas group (Moustakas *et al.*, 1985) and *p*-type μc-Si:H layer by Fang group (Fang *et al.*, 1982) followed by the development of tandem solar cells where a layer of nc-Si:H and a layer of a-Si:H is used as the intrinsic layer in a p-i-n solar cells to optimize the light efficiency of the cell (Moustakas *et al.*, 1985). Willeke group

demonstrated that nc-Si:H films could be deposited at low temperatures (<150°C), opening the opportunity for electronics on flexible substrates using μc-Si:H thin films (Willeke *et al.*, 1988).

The term μc-Si:H refers to films with Si crystals of size above 100 nm and at the turn of the century, the term hydrogenated nanocrystalline silicon (nc-Si:H) emerged as the size of the Si crystals embedded within the amorphous matrix decreased to less than 100 nm. Nanocrystalline silicon is similar to a-Si:H except that it contains very small Si nanocrystals or nanocrystallites embedded within the amorphous silicon matrix. These crystallites, or crystalline grains of Si, are usually about tens of nanometers in size (Svrcek *et al.*, 2001). These crystallites are surrounded by grain boundaries which are saturated by hydrogen or with thin hydrogenated amorphous silicon (a-Si:H) tissue. The nc-Si:H showed some of advantages over a-Si:H such as higher mobility and greater stability against light induced degradation. At the same the nc-Si:H demonstrated improved electrical characteristics compared to a-Si:H such as low leakage current and possibility of fabricating high quality p-type material. Since the Si grains in nc-Si have a band gap closer to the single c-Si band gap of 1.1 eV (a-Si:H has a band gap of around 1.7 eV), it is currently being used in thin film solar cell research, to improve the efficiency of solar cells by absorbing more red and infrared light. Nanocrystalline silicon films also exhibit visible to infrared photoluminescence (PL) spectrum at room temperature due to quantum confinement of electrons in the Si nano-crystallites embedded within the amorphous silicon matrix.

1.3 Photoluminescence Emission from Silicon Nanostructures

Silicon is the key material for nanomaterials science since it is an element semiconductor and there is no composition fluctuation even in very small nanostructures. Silicon nanostructures can be classified into four types: (i)

nanocomposites [3D], (ii) quantum wells [2D], (iii) nanowires and nanotubes [quasi 1D], and (iv) nanoparticles and quantum dots [(quasi) 0D]. Many unique Si-based nanostructures and nanomaterials have been fabricated such as nanocrystalline silicon, Si clusters, Si nanoparticles, Si nanowires and so on. Well-controlled Si nanostructures have potential applications for quantum device applications and molecular electronics. Quantum confinement, spatial confinement and surface effects have been shown to be the origin of PL emission in c-Si and a-Si based nanostructures (Song *et al.*, 1998; Tong *et al.*, 1999; Qin *et al.*, 1995). PL emission in a-Si nanostructures is caused by quantum confinement of carriers and short carrier lifetime in the band-tail states. Surface oxidized and H-passivated c-Si nanoparticles have been shown to have different PL mechanism. Light absorption and light emission occur in the c-Si core state in hydrogen-passivated nanostructures while in oxidized Si nanocrystals, light absorption occurs in the core state and light emission occurs in the oxygen modified states between the c-Si and the SiO surface layer (Dinh *et al.*, 1996).

1.4 Current and Potential Applications

Most studies on applications of silicon nanostructures are concentrated on nc-Si:H thin films and this material has found promising applications in solar cells, thin films transistors (TFTs), displays and other devices (Orpella *et al.*, 2001; Photopoulos *et al.*, 2000; Sato and Hirakuri, 2006). It has the advantage of being stable under Staebler-Wronsky effect and has higher diffusion length, carrier mobility and conductivity compared to a-Si:H. The photoluminescence (PL) emission from nc-Si:H films makes it attractive for applications in optoelectronics integrated into standard silicon VLSI technology as well as in thin film solar cells for additional carriers generation (Iacona *et al.*, 2000; Linnros *et al.*, 1999; Canham, 1990). In order to enhance quantum confinement effects in nc-Si:H for enabling band gap spreading for PL emission, Si

nano-crystallites have to be embedded into insulating matrix (Gudovskikh *et al.*, 2004). The insulating matrix used to embed the Si nano-crystallites includes amorphous silicon (Parashar *et al.*, 2010), silicon oxide (Benyoucef and Kuball, 2001; Jeon *et al.*, 2005) or silicon nitride (Kim *et al.*, 2004) matrix.

The high surface to volume ratio and aspect ratio in the form of quantum dots and nanowires (NWs) respectively demonstrate effective light emission ability in the visible and near infrared region and are promising material for nano-scale optoelectronic devices. Low optical reflectance and high optical absorption over all wavelengths of Si NWs are properties that are expected to enhance the properties of nanostructure solar cells (Tsakalakos, 2008). Si NWs-based solar cells have been proposed (Tsakalakos *et al.*, 2007; Bayes *et al.*, 2005) and CVD grown NWs have added advantage of direct growth on flexible substrates and improved cost benefit compared to bulk Si solar cells owing to lower material consumption since only gases are used for fabricating the active material.

Si quantum dots (QD) and nanoparticles (NP) have also been implemented in various applications including photovoltaics (Wu *et al.*, 2005), biological labelling applications (Alivisatos *et al.*, 2005), nanoelectronic applications (Cui *et al.*, 2004). Si quantum dots (QD) and nanoparticle s(NP) have been coated with dielectrics like SiO or SiN or additional semiconductors to create core-shell nanostructure for many of these application (Qi and Lee, 2009; Pei and Hwang, 2003; Zhang *et al.*, 2007). Several Si quantum dot-based solar cell designs have been proposed in literature. Green and co-workers proposed the use of multi-layered Si quantum dots arrays to create an all Si-based Si quantum dot multi-junction solar cells (Connibeer *et al.*, 2006). Another group,M. Ficcadenti *et al*. deposited thin film stacks, made of Si-rich SiO alternated with SiO_2 layers by reactive RF sputtering starting from Si and SiO_2 targets, respectively to grow crystalline quantum dots by Si precipitation from the Si-rich SiO

phase using high temperature annealing for solar cell fabrication (Ficcadenti *et al.*, 2009). The use of Si NPs in bio-labeling and bio-sensing applications has also been proposed by various researchers. Oillic and co-workers used Si nanostructures prepared by CVD process to improve the sensitivity of fluorescence detection in DNA arrays (Oillic *et al.*, 2007). In 2007, Zhang group demonstrated promising approach to improve the electrochemical performance of nano anode material for lithium battery by using core-shell Si/SiO nanocomposite. These potential and promising applications of Si nanostructures have created the increase in interest in Si nanostructures research as shown in Figure 1.1.

1.5 Focus and Motivation of Research

The approach of layer-by-layer (LBL) technique of depositing microcrystalline silicon (μc-Si) using plasma enhanced chemical vapour deposition (PECVD) was followed in this thesis. In this technique hydrogenated silicon (Si:H) deposition was alternated with hydrogen plasma treatment to control the growth process. P. Roca I Cabarocas and co-workers (Cabarocas *et al.*, 1996) reported that this technique was able to convert a-Si:H film into μc-Si film and the nucleation of crystalline phase occurred within a highly porous a-Si:H material. Hamma (Hamma and Cabarocas, 1998) also from the same group used similar technique but added argon to hydrogen during the hydrogen plasma treatment. Dense and highly crystalline μc-Si grown on a-Si:H substrates were obtained at low substrate temperatures. Houben and co-workers (Houben *et al.*, 1998) used very high frequency (VHF) PECVD to compare the morphology of μc-Si films grown by continuous deposition (CD) and LBL deposition. They used hydrogen diluted silane during the film growth process instead of pure silane as done by Cabarocas group (Cabarocas *et al.*, 1996; Hamma and Cabarocas, 1998). They showed that CD and LBL growth of μc-Si films on non-crystalline substrates led

similar microstructural features. Lin group (Lin *et al.*, 2006) studied the structure and morphology of films grown by LBL technique using rf PECVD. They used similar LBL technique as L. Houben *et al*. where silane diluted in hydrogen was used during the film growth cycle but was done in rf powered plasma. Nanocrystalline silicon (nc-Si) films with high mobility and high absorption in the visible region suitable for fast photodetecting applications were produced.

A home-built rf PECVD system was developed for this work to grow hydrogenated nanocrystalline silicon (nc-Si:H) films from silane (SiH_4) and hydrogen (H_2) gases. It is well established that the properties of nc-Si:H films grown by any CVD techniques are strongly dependent on the deposition parameters. Optimisation has to be done to get a better understanding on the growth conditions and plasma conditions that would result in films with the properties for the desired applications of these films. The growth conditions and plasma conditions of nc-Si:H films prepared by CD using rf PECVD technique are quite established since these have been widely researched on especially in the last decade. Therefore, these reported results can be used to establish whether the properties of the films produced by the home-built system with respect to important deposition parameters like rf power, substrate temperature and hydrogen to silane flow-rate ratio are consistent with the reported results. Since the LBL deposition of Si:H films has not been investigated much except for the works reported by the above named groups. Therefore, the novelty of this work has been shown to be able to control the growth process of μc-Si and nc-Si films, by the LBL deposition using this newly developed rf PECVD system for growing well-controlled silicon nanostructures with light emitting properties. Since the origin of PL emission in Si based films has been reported to be due to quantum confinement, spatial effects or surface effects (Wang *et al.*, 2005), it is important to produce Si nanostructures with a Si nano-crystallites embedded in amorphous Si matrix (a-Si) or mixed phases of a-Si or

amorphous SiO. The hydrogen plasma treatment on the oxide layer and also during the growth process of the c-Si substrate is expected to diffuse the oxygen atoms through the growth layers to form the SiO phase. The controlled growth process of LBL technique is expected to be able to control the crystallite size, crystalline volume fraction and the SiO component in the amorphous matrix in the Si nanostructures with light emission properties.

The aim of this PhD work is to grow Si nanostructures with PL emission properties by LBL deposition technique using rf PECVD system. However, in order to achieve this objective the influence of very important deposition parameters on the growth rate, optical, chemical bonding and structural properties of Si:H films grown by CD and LBL deposition techniques using a PECVD deposition system specially designed and built for this work are studied and compared. These films are grown at different rf powers, substrate temperatures and hydrogen to silane flow-rate ratios on both c-Si and glass substrates. The influence of substrates on these properties is also investigated. The characterization of the samples for this part of the work is performed using in-house characterization systems which include the ultra-violet visible near-infrared (UV-VIS-NIR) spectrophotometer, Fourier transform infrared spectrometer (FTIR) and X-Ray diffractometer (XRD). This part of the work is also done to establish that LBL deposition of Si:H films is capable of producing highly crystalline films on c-Si substrates which is anticipated to have light emission properties. The deposition parameters which produced significant influence on the crystallinity of the Si:H material are also identified for the next part of the work. The second part of the work is concentrated on the study of the morphology, crystallinity, crystallite size and silicon-oxygen bonding properties of the Si:H material grown on c-Si substrates by LBL technique in relation to the parameters identified at the end of the first part of the work. The silicon-oxygen bonding properties are extracted from the FTIR spectra of the films.

Micro-Raman scattering spectroscopy, field emission scanning electron microscopy (FESEM), high resolution transmission electron microscopy (HRTEM) and Micro-Photoluminescence spectroscopy (PL) characterization techniques are used to study the morphology, structural and photoluminescence properties of the material. These characterization techniques are not available in-house and therefore have to be done at various institutions in Malaysia and Singapore where these facilities are available. The deposition mechanism and structural configuration of the material grown will be proposed based on the analysis of the studies on morphology, crystallinity, crystallite size and silicon-oxygen bonding properties of the material. Lastly, the influence of these properties on the PL emission properties of the material is investigated

Objectives of the Work

1. To grow Si nanostructures with PL emission properties by LBL deposition technique using home-built PECVD deposition system,
2. To study and compare the growth rate, optical, chemical bonding and structural properties of Si:H thin films grown by CD and LBL deposition techniques using a home-built PECVD deposition system at different optimized deposition conditions,
3. To study the influence of substrates on the properties of the Si:H thin films,
4. To study the morphology, crystallinity, crystallite size and silicon-oxygen bonding properties of the Si:H thin films grown on c-Si substrate by the LBL deposition technique,
5. To relate the properties of the nanostructures with the PL emission properties,
6. To propose a growth mechanism and structural configuration of the Si nanostructures based on the previous studied of the properties of the films.

1.6 Outline of the Thesis

In order to identify issues that are important to this research the relevant literature related to this work are reviewed in Chapter 2. This chapter begins with a review on the deposition techniques and the growth mechanism of nc-Si:H thin films compiled from various published reports. This is followed by a detailed discussion on the influence of deposition parameters on the properties of nc-Si:H thin films produced by PECVD. Subsequently, a review on the dependence of growth rate of nc-Si:H thin films on the deposition parameters is presented. The chapter ends with discussions on the optical and structural properties of nc-Si:H thin films and how deposition parameters influence these properties.

Chapter 3 describes the sample preparation technique and the analytical techniques used to study the properties of nc-Si:H thin films in this work. Section 3.2 describes in detail the rf PECVD system, sample cleaning procedures and LBL deposition technique. Section 3.3 describes the analytical techniques used to characterize the optical, structural and surface morphological of nc-Si:H thin films deposited by LBL deposition technique. This section also includes physical principles, instrumentation and calculation methods used to analyze the results obtained from the characterisation done on the samples.

Chapter 4 discusses the results of optical and structural properties of Si:H thin films deposited by LBL and CD techniques using a home-built rf PECVD system at different deposition conditions. The effects of rf power, substrate temperature and hydrogen to silane flow-rate ratio, on the properties of the films deposited on c-Si and glass substrates by LBL and CD techniques are discussed and compared. The influence of substrate used on the properties of the films is also discussed when characterization is done on films deposited on both c-Si and glass substrates.

Chapter 5 is focused on the crystallinity, surface morphology, microstructure and photoluminescence emission properties of nc-Si:H thin films deposited on c-Si substrates by LBL deposition technique using a home-built rf PECVD system. The effects of the deposition conditions on these properties are discussed. The relation between crystallinity, surface morphology and microstructure of the films with PL emission under the effect of deposition conditions are also discussed. Based on the results, this chapter ended with a proposal of the growth mechanism of nc-Si nanostructures. Finally, Chapter 6 concludes the research findings that have been discussed in Chapters 4 and 5 with some suggestions for further work.

Chapter 2

Literature Review

2.1 Introduction

As stated in Chapter 1, hydrogenated nanocrystalline silicon (nc-Si:H) thin films are a mixed-phase of Si nano-crystallites embedded within an amorphous matrix. Extensive studies have been recently carried out in order to understand the properties of this mixed-phase material, mainly in optoelectronic applications, such as solar cells, thin film transistors (TFTs) and sensors. A review of previous works on the deposition and properties of nc-Si:H, indicate that is important to familiarise yourself with this material in order to produce a better quality of nc-Si:H.

This chapter begins with a description of various favourable deposition techniques used to produce nc-Si:H thin films. The next section gives a detailed description of the growth mechanisms of nc-Si:H, including the gas phase reactions and the film-growth process on the surface of the film. This leads to an understanding of the formation of Si nano-crystallites during the nucleation growth. The properties of nc-Si:H thin films strongly depend on the Si nano-crystallites embedded in the amorphous structure. The section continues with a review of the role of the deposition parameters in the deposition of nc-Si:H thin films. The chapter ends with a review of structural and optical properties of nc-Si:H thin films.

2.2 Deposition Techniques of Hydrogenated Nanocrystalline Silicon (nc-Si:H) Thin Films

Hydrogenated nanocrystallie silicon (nc-Si:H) thin films can be produced using various deposition techniques, such as plasma enhanced chemical vapour deposition (PECVD) (Bhattacharya and Das, 2007; Chen et al., 2008), hot wire chemical vapour deposition (HWCVD) (Waman *et al.*, 2011; Bakr *et al.*, 2011), radio-frequency (rf) magnetron sputtering and electron cyclotron resonance chemical vapour deposition (ECR-CVD). Among these techniques, the PECVD is the most favourable and

promising deposition technique for large area thin film technology and has been employed for industrial applications because of its simple deposition technique.

2.2.1 Plasma Enhanced Chemical Vapour Deposition (PECVD)

The chemical vapour deposition (CVD) method involves the deposition of gaseous reactants on a heated surface. In CVD, the critical step in deposition is the thermal activation, since this often requires high temperatures for a chemical reaction to take place (Lieberman and Litchenberg, 1994). This limiting factor can be overcome by creating an electric discharge or glow discharge plasma. A glow discharge is a manifestation of the electrical conduction through gases (Llewellyn-Jones, 1966) in the reactant gases to produce a large number of free radicals and ionic species. This technique is known as Plasma Enhanced Chemical Vapour Deposition (PECVD).

The PECVD process is based on the decomposition of a gaseous compound into radicals, atoms and ions near the substrate surface. One of the reaction products is a solid, which precipitates onto the surface to form a new layer of thin film. The decomposition of gas compounds depends on the form of excitation used to create the discharge. This technique has been most widely used for depositing nc-Si:H by decomposition of silane (SiH_4) and hydrogen (H_2) in glow discharge plasma, which is generated by a radio frequency (RF) of a 13.56 MHz power source. The advantage of the plasma over the CVD is its capability of a low temperature preparation of the crystalline silicon because of the nonequilibrium process. In PECVD, the film deposition is possible even at room temperature, because the decomposition of the source gas as SiH_4 is caused by energetic electrons.

2.2.1(a) Radio-frequency Plasma Enhanced Chemical Vapour Deposition (rf PECVD)

The phrase rf PECVD refers to the configuration of a rf glow discharge when an rf electric field is applied to the cathode electrode in a gaseous medium in a vacuum chamber under controlled pressure. A diode reactor, which consists of two electrodes, a powered electrode and a ground electrode, is usually used in the deposition of nc-Si:H thin films. In this reactor, the substrate is usually placed on the grounded electrode. Because of this asymmetric geometry and the fact that the electron mobility is much larger than the ion mobility (Chapman, 1980; Kasper *et al.*, 1992), the two electrode regions will have different amounts of potential drop, which accelerates ions toward the electrodes and electrons, away from the electrodes. The larger potential drop appears at the power electrode, which is more negative with respect to the grounded electrode, as shown in Figure 2.1. This is the reason why the powered electrode is often called the cathode and the grounded electrode is called the anode. The rf frequency of 13.56 MHz is a standard frequency allotted by international communications authorities, at which one can radiate a certain amount of energy without interfering with communications.

In the figure, the ground potential is always negative with respect to the plasma potential and therefore the substrate's surface on the grounded electrode suffers the bombardment by positive ions. The powered electrode is even more negative with respect to the plasma and thus subjected to even more positive ion bombardment than the anode. The plasma glow region is the place where the potential is near the plasma potential, which is where most of the inelastic electron-impact gas dissociation takes place. The dark region between the boundaries of the glow region and the electrodes is called the sheath or dark space. Increasing power increases the sheath voltage but decreases the sheath widths (Jansen *et al*. 1985). For rf discharge, the plasma sheath near the grounded electrode with the substrate contributes to the generation of more neutral radicals close to the electrode, improving the deposition rate. However,

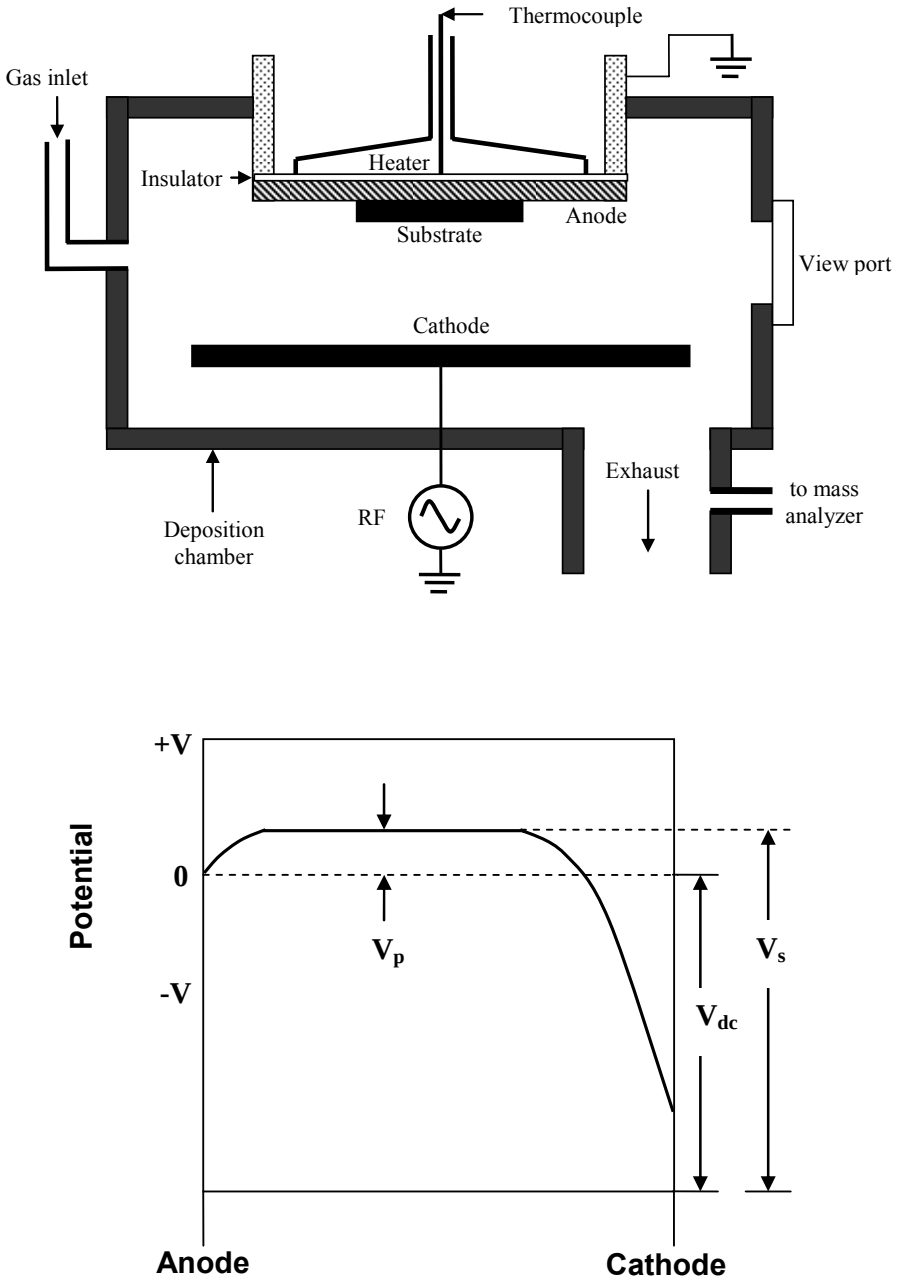

Figure 2.1: Spatial distribution of average potential in RF-powered diode reactor. V_p, V_{dc} and V_s represent plasma potential, average self-bias and sheath potential.

increasing power accelerates the positive ions toward the substrate and give rise to the ion bombardment. The plasma potential of the rf discharge of SiH_4 is of the order of 10 eV and the ion energy can be varied by applying the substrate bias.

In order to improve the uniformity of the film thickness and material properties, the source gas is often supplied from the cathode electrode, such as in a showerhead electrode configuration. The hydrogen dilution is a crucial parameter in determining the structure. As has been reported, the hydrogen dilution ratio has a threshold for crystal growth, and by increasing the hydrogen dilution ratio, the crystallinity is improved (Matsuda, 1983).

Although rf PECVD is technically expensive and difficult to set up with impedance matching problems, nevertheless this technique is widely used because RF is more efficient than its dc counterpart in promoting ionization and sustaining the discharge, since electrons gain higher energies as they follow oscillatory paths between the electrodes. Rf also gives the ability to bombard insulating surfaces, since the oscillating electrons do not reach the electrodes and no real current flows through the circuit, compared to dc PECVD.

2.2.2 Hot-Wire Chemical Vapour Deposition (HWCVD)

The HWCVD, formerly called Catalytic-CVD or Cat-CVD, is a technique that involves the decomposition of silane or silane/hydrogen mixtures at a resistively heated filament, which is used to produce thin films of polycrystalline and amorphous silicon at relatively low temperatures on various substrates. This technique was first introduced and patented in 1979 as thermal CVD by Wiesmann *et al*., 1979, who made use of a tungsten or carbon foil that was heated to a temperature of 1400 – 1600°C. At such temperatures, thermal decomposition of silane into gaseous mixtures of hydrogen and silicon atoms was thought to take place. Recently, this technique has been used to

deposit a high deposition rate of microcrystalline silicon thin films with a desirable crystalline volume fraction (Jadkar *et al.*, 2000).

The principle of HWCVD is that the feedstock gas, such as silane, is decomposed effectively into atomic fragments at the surface of the filament at temperatures above 1500°C.

$$SiH_4 \rightarrow Si + 4H, \qquad (2.1)$$

In contrast to the conventional PECVD technique, there are no ions created. Although the hot filament emits a considerable electron current, the energy of these electrons is too low to cause any impact ionization.

A schematic cross section of an HWCVD set up is shown in Figure 2.2 (Schropp and Zeman, 1998). The substrate is placed a few centimetres away from the filament. The wire used as the hot filament is made of tungsten or tantalum and has a thickness of between 0.25 and 0.5 mm. The wire is heated by a d.c. or an a.c. current. The wire temperature is preferably kept between 1750 and 1950°C. Lower temperatures lead to the formation of tungsten silicide on the wires, thus reducing the catalytic action of the hot filament. Higher temperatures lead to the evaporation of the tungsten wire itself and subsequent detectable tungsten incorporation into the film. By employing a proper multi-wire arrangement it is possible to obtain a good thickness uniformity over a large area. The wires are acting as true line sources (Feenstra *et al.*, 1997). In combination with a low pressure, this enables a high deposition rate without gas-phase nucleation of particles. If the pressure is too high or the substrate-filament distance is too large, the film properties will be inferior due to significant gas phase polymerization.

2.2.3 Radio-frequency (rf) Magnetron Sputtering

Sputtering is one of the alternative techniques to prepare nc-Si:H, from sputtering of a silicon target in a mixture of inert gas, which usually involves argon gas,

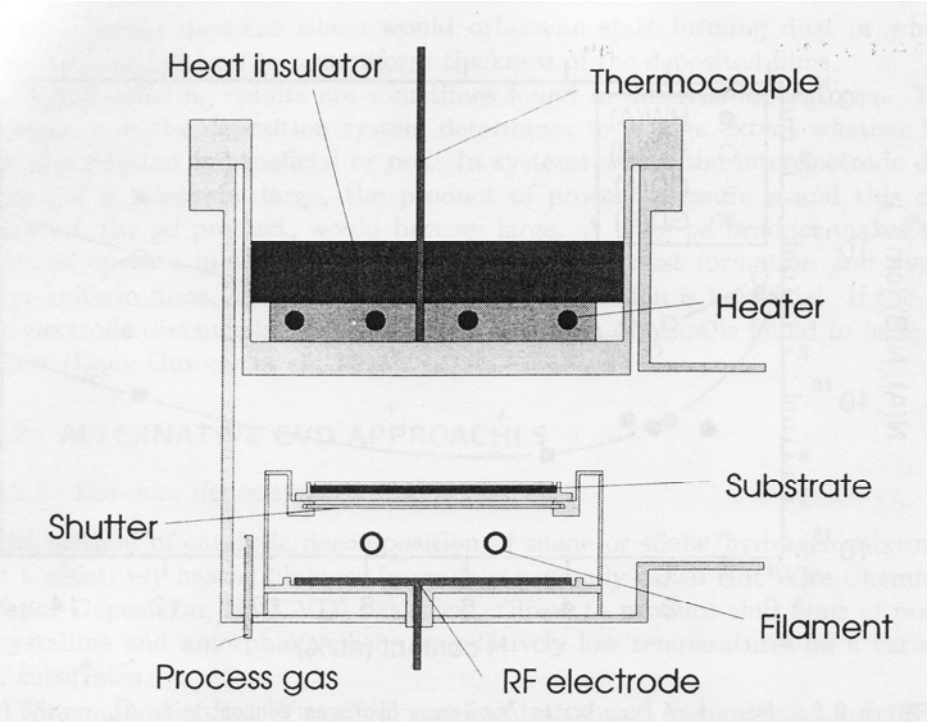

Figure 2.2: Schematic cross section of an HWCVD reactor. The same chamber can be used for PECVD (Schropp and Zeman, 1998).

and hydrogen. Figure 2.3 shows a schematic diagram of a sputtering vacuum system (Vossen, 1978). This deposition technique has the ability to uncouple the two source materials, Si and H, and independently optimize the role that each plays in forming the network and in determining the ensuing electro-optical properties. This type of control is not possible for the glow discharge decomposition of silane, because the source materials are initially chemical bonded in the feed gas of SiH_4. In addition, sputtered films in general are mechanically strong (good film – substrate adhesion) and the process is easily scalable. However, there are a few crucial disadvantages, which have led to this technique not being favourable for the depositing of nc-Si:H films. This process is favourable at a high partial pressure of hydrogen ($H_2/Ar \geq 1$) and at low sputtering rates. Furthermore, the hydrogen plasma may react with the surface of the target and form volatile SiH_x compounds in the hydrogen etching processes. Lastly, the ion bombardment may damage and possibly disorder the surface of the target.

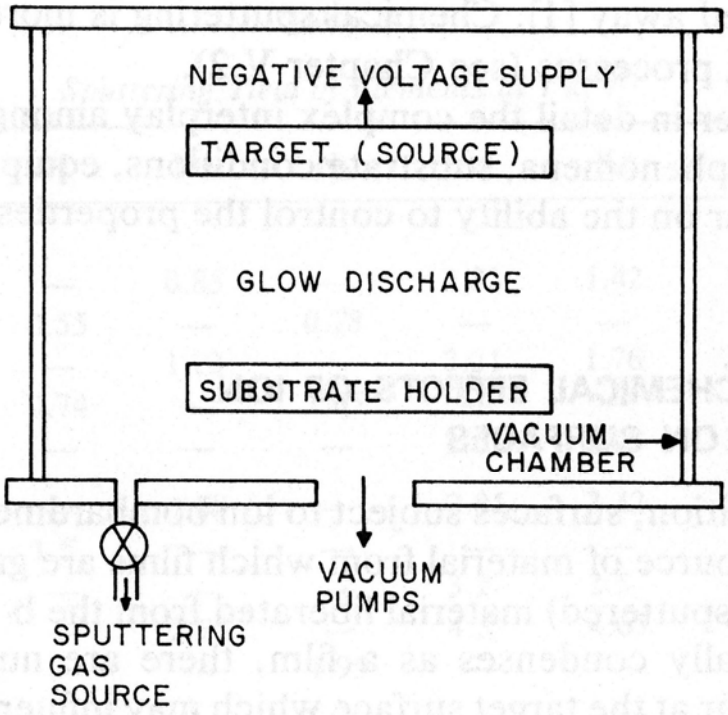

Figure 2.3: Schematic cross section of a sputtering system (Vossen, 1978).

2.2.4 Electron Cyclotron Resonance CVD (ECR-CVD)

The ECR-CVD technique is, in fact, a remote-plasma CVD technique (Ichikawa *et al*., 1987). Figure 2.4 shows a schematic diagram of an ECR-CVD reactor (Shing, 1989). Plasma is generated in a carrier gas, such as Ar, He or H_2, by microwave excitation (usually 2.45 GHz) in a remote chamber. Due to an externally applied magnetic field, the electrons achieve cyclotron motion, and by tuning the field strength, B, the frequency of the electrons $\omega = {eB}/{m}$ is brought at resonance with the microwave frequency. Thus, the remote plasma chamber acts as a resonance cavity, and hence the technique is called Electron Cyclotron Resonance CVD. The microwave power is effectively transferred to the plasma. The plasma is characterized by a high density of high energy electrons, which leads to a high dissociation rate, while the gas temperature is low. The plasma is able to sustain at a pressure as low as 1 mTorr.

The feedstock silane is introduced at a location near the substrate. As the magnetic field diverges into the deposition chamber, an electric field is generated in the plasma column, and ionized radicals (SiH_n^+) from the plasma are driven to the substrate, where they bombard the growing surface. Due to the high frequency, a large ion flux with a sufficiently low energy enhances the deposition rate, which preserves the material quality. The large ion flux allows the use of low substrate temperature. The ion energy can be controlled by gas pressure. Due to the significant ion energy transfer to the substrate, ECR-CVD is suitable for highly conductive microcrystalline doped layer deposition (Hattori *et al*., 1987).

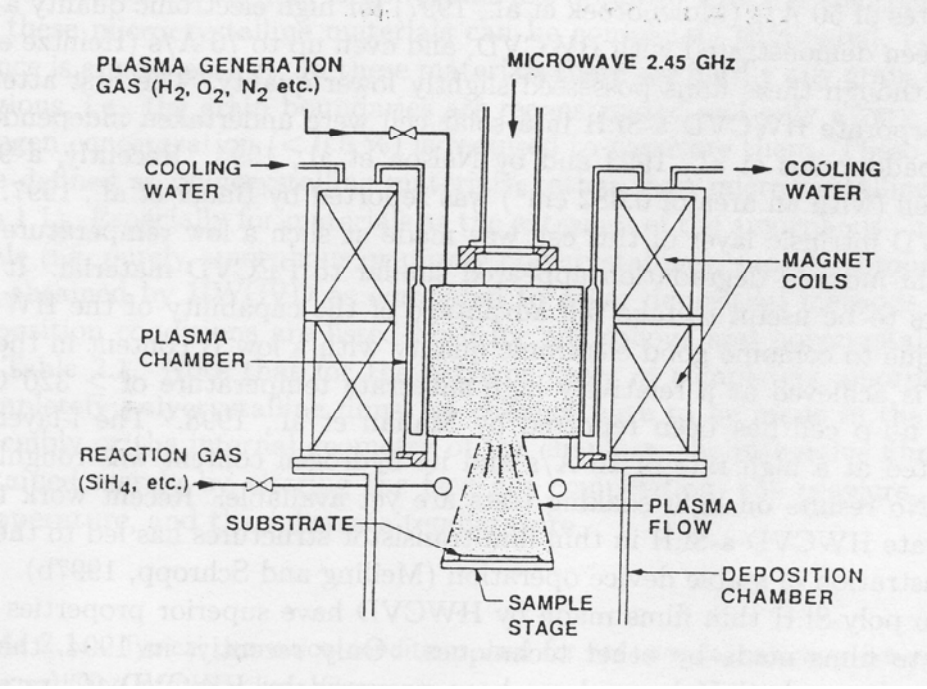

Figure 2.4: Schematic diagram of an ECR-CVD reactor (Shing, 1989).

2.3 Understanding of nc-Si:H Growth

Nc-Si:Hs prepared from a silane and hydrogen mixture using PECVD are being widely used due to their high potential for preparing high quality materials uniformly on a large area substrate at low substrate temperature (around 200-400°C). Silane plasmas

have been extensively studied with respect to the plasma processes (primary and secondary reactions), the surface reaction and the material properties as shown in Figure 2.5 (Cabarrocas *et al.*, 2002). Generally, the SiH_3 has been reported as a growth precursor to produce a low defect density of nc-Si:H. However, the SiH_3 must be accompanied by specific substrate temperature conditions (150-250°C) in order to provide mobility to the radicals on the surface and promote cross-linking reactions leading to the elimination of excess hydrogen, to conclude with typically 10 % atomic hydrogen in the film (Street, 1991). However, by increasing the deposition rate, which can be achieved by increasing the RF power, the pressure in the reactor, as shown in Figure 2.5, will result in the formation of powder, and eventually deteriorate the material properties. Recently, the Cabarrocas Group has reported that polymorphous silicon (pm-Si:H) produced at the onset of the powder formation showed high optical absorption while having improved electronic and transport properties (Cabarrocas *et al.*, 2002; Kleider *et al.*, 1999). In this section, we discuss the growth mechanism of the low temperature growth of nc-Si:H in the gas phase reaction, as well as the surface reaction, particularly focusing on the role of atomic hydrogen and ion bombardment.

2.3.1 Gas phase reactions - Primary and secondary reactions in SiH_4/H_2 plasmas

The initial step for the growth of nc-Si:H is the decomposition process of the source gas materials in the SiH_4/H_2 glow discharge plasma. Figure 2.6 shows a schematic sketch of the dissociation pathway of SiH_4 and H_2 through electronic excited states of those molecules by inelastic collisions with high energy electrons in the plasma (Matsuda, 2004). As the energy of electrons in the plasma varies from zero to several ten electron volts (eV), the ground state electrons of the source gas molecules are excited into their electronic excited states almost simultaneously by inelastic collisions with energetic electrons. Electronic excited states of complicated molecules like SiH_4

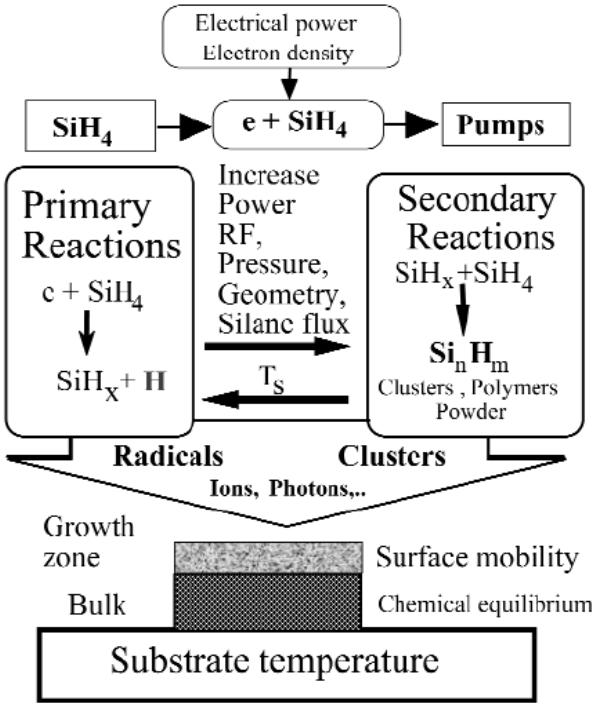

Figure 2.5: Schematic representation of the processes involved in amorphous silicon deposition (Cabarrocas et al., 2002).

are usually dissociating states, from which dissociation occurs spontaneously to SiH_3, SiH_2, SiH, Si, H_2 and H, as shown in Figure 2.6, depending on the stereo-chemical structure of excited states, without emitting photons to return to their ground states (Tsuda *et al.*, 1989). Hydrogen molecules are also decomposed to atomic hydrogen. Excitation of ground state electrons to the vacuum state causes ionization events, producing new electrons and ions to maintain the plasma.

Reactive species produced in the plasma experience secondary reactions mostly with the parent SiH_4 and H_2 molecules, as shown in Figure 2.7, forming a steady state. The reaction rate constants for each reaction are summarized in the literature (Perrin *et al.*, 1996). Steady state densities of reactive species are determined by the balance between their generation rate and their annihilation rate. Therefore, highly reactive species, such as SiH_2, SiH and Si, with SiH_4 and H_2 (short lifetime species), take on

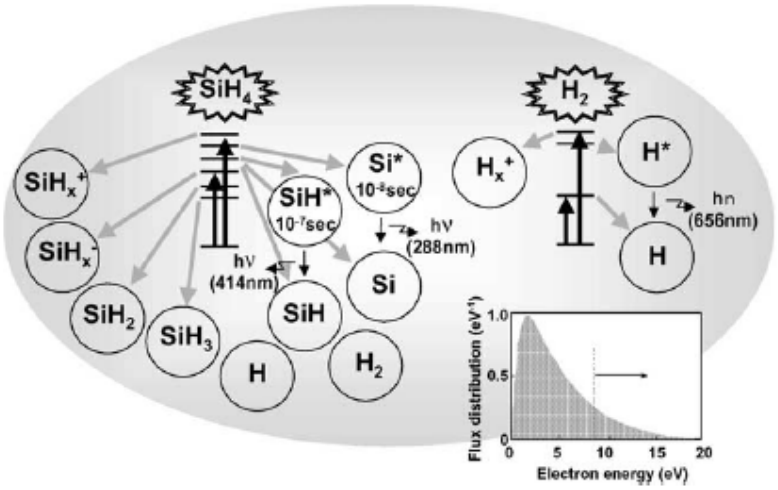

Figure 2.6: Schematic concept for the dissociation processes of SiH_4 and H_2 molecules to a variety of chemical species in the plasma through their electronic excited states. Electron energy distribution function in the plasma is also shown (Matsuda, 2004).

Ion exchanging	$SiH_x^+ + SiH_4 \rightarrow SiH_x + SiH_4^+$
Ion - Molecule	$SiH_x^+ + SiH_4 \rightarrow SiH_3^+ + SiH_3$
Neutral - Molecule	$SiH + SiH_4 \rightarrow Si_2H_5$
disproportionation	$Si + SiH_4 \rightarrow SiH_3 + SiH$
insertion	$SiH_2 + SiH_4 \rightarrow Si_2H_6$
recombination	$SiH_2 + H_2 \rightarrow SiH_4$
abstraction	$SiH_3 + SiH_4 \rightarrow SiH_4 + SiH_3$
	$H + SiH_4 \rightarrow H_2 + SiH_3$
Ion - Radical	less probable
Radical - Radical	less probable

Figure 2.7: Representative secondary reactions of chemical species produced in the plasma with SiH_4 and H_2 molecules. Their reaction rate constants are available from the literature (Perrin *et al.*, 1996).

much smaller values than SiH_3, showing no reactivity with SiH_4 and H_2 (short lifetime species) in the steady state plasma, although the generation rates of those species are not so different.

Steady state densities of reactive species in the plasma have been measured using various gas-phase diagnostic techniques (Itabashi *et al.*, 1990a; Itabashi *et al.*,

1990b; Tachibana *et al.*, 1991; Matsuda and Tanaka, 1982; Matsuda *et al.*, 1980; Matsumi *et al.*, 1986; Kono *et al.*, 1995), such as optical emission spectroscopy (OES), laser induced fluorescence method (LIF), infrared laser absorption spectroscopy (IRLAS) and ultra-violet light absorption spectroscopy (UVLAS), as well as other techniques. Figure 2.8 shows the steady state number densities of chemical species including emissive and ionic species in SiH_4/H_2 realistic plasmas (Matsuda, 2004). It can be clearly seen in the figure that SiH_3 radicals are the dominant chemical species, although the density ratio of the short lifetime species to SiH_3 varies when changing the plasma generation conditions. For instance, when high electric power (high electron density) is applied to the plasma under low SiH_4 flow-rate condition, SiH_4 is highly dissociated, followed by a depletion, resulting in the reduction of the gas phase reaction probabilities of short lifetime species with SiH_4 molecules, leading to an increase of the contribution ratio of short lifetime species to the film growth, which causes a deterioration of structural properties in the resulting films.

Steady state density of atomic hydrogen (H) takes a wide variety in the plasma, also shown in Figure 2.8. This is mainly due to the change in the hydrogen dilution ratio, R (H_2/SiH_4) in the starting source gas materials, i.e., the density of atomic hydrogen increases with increasing R. When consideration the fact that nc-Si:H is formed with increasing R at a constant electron density in the plasma and at a constant substrate (surface) temperature, it suggests that atomic hydrogen plays an important role in the film growth.

2.3.2 Film-growth process on the surface

In the conventional growth mechanism of a-Si:H that was proposed by A. Matsuda (Matsuda, 2004), SiH_3 radicals reaching the film-growing surface start to diffuse on the surface. During surface diffusion, SiH_3 abstract the hydrogen from the

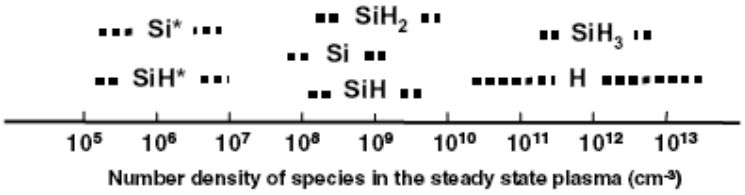

Figure 2.8: Number density of chemical species in the realistic steady-state plasmas measured or predicted by various diagnostic techniques (Matsuda, 2004).

surface covering by bonded hydrogen, forming SiH_4 and leaving dangling bonds on the surface (growth site formation). The dangling-bond site and the Si-Si bond (film growth) are schematically shown in Figure 2.9.

Three predominant models that were proposed by Matsuda on the growth mechanism of μc-Si:H have been used to understand the formation of nc-Si:H. The three models consist of the surface diffusion model (Matsuda, 1983), the etching model (Tsai *et al*, 1989) and the chemical annealing model (Nakamura *et al.*, 1995).

The surface diffusion model is schematically depicted in Figure 2.10(a). A large amount of atomic H flux from the plasma produces a full surface coverage by bonded hydrogen and produces local heating through hydrogen exchanging reactions on the film growing surface. These two actions enhance the surface diffusion of the film precursors (SiH_3). As a consequence, SiH_3 adsorbed on the surface can find energetically favourable sites, leading to the formation of an atomically ordered structure (nucleus formation). After the formation of the nucleus, the epitaxial like growth takes place with an enhancement of surface diffusion of SiH_3 (Matsuda, 1983; Matsuda, 1999). In the growth of a-Si:H, a-SiGe:H and a-SiC:H, this model successfully accounts for the surface smoothing effect and the improvement of film quality under the hydrogen dilution condition (Matsuda and Tanaka, 1987; Ganguly and Matsuda, 1993).

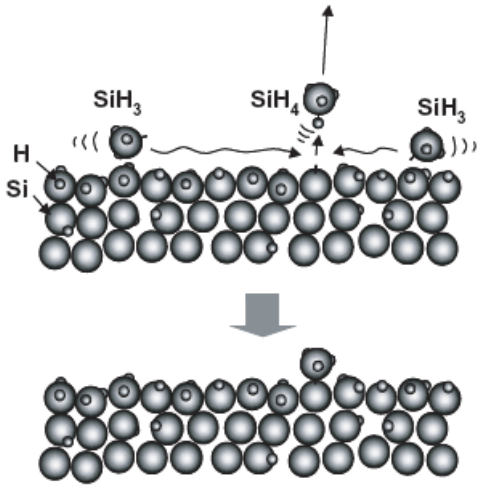

Figure 2.9: Schematic sketch for the surface growth process of a-Si:H.

The etching model was proposed based on the experimental fact that the chemical transport mechanism contains a critical balance between the etching rate and the growth rate on the growing surface. In fact, the growth rate is reduced with an increase of the hydrogen dilution ratio, *R* to the critical balance point. A concept of the etching model is schematically shown in Figure 2.10(b). Atomic H reaching the film growing surface break the Si-Si bonds, preferentially weak bonds involved in the amorphous network structure, leading to a removal of Si atoms weakly bonded to another Si. This site is replaced with a new film precursor, SiH_3, creating rigid and strong Si-Si bonds, resulting in an ordered structure (Tsai *et al*., 1989; Matsuda, 1999).

The chemical annealing model was proposed to explain the experimental fact that a crystal formation is observed during the hydrogen plasma treatment in a layer-by-layer growth by an alternating sequence of thin amorphous film growth and hydrogen plasma treatment. Several monolayers of amorphous silicon are deposited and these layers are exposed to hydrogen atoms produced in the hydrogen plasma. These procedures are repeated alternately for several ten times to fabricate the proper thickness for evaluation of film structure. The absence of a remarkable reduction of film thickness during the hydrogen plasma treatment is hard to explain by the etching model,

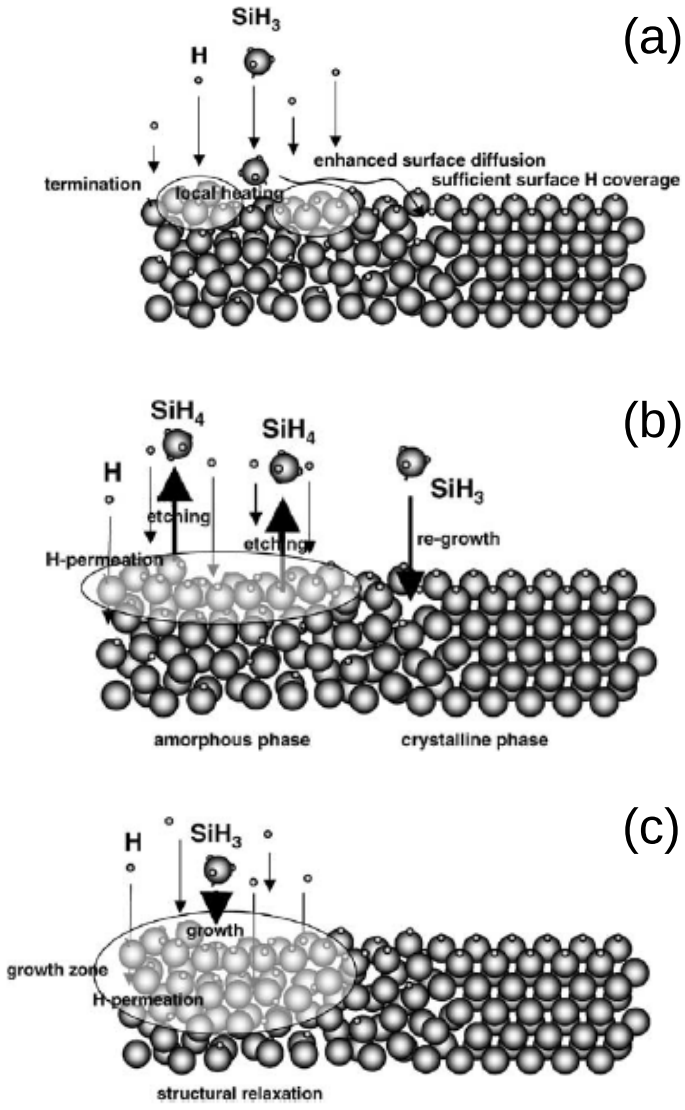

Figure 2.10: (a) Surface diffusion model for nc-Si:H formation. Large spheres and small spheres represent Si and H, respectively. (b) Etching model for nc-Si:H formation. (c) Chemical annealing model for nc-Si:H formation (Matsuda, 2004).

and the chemical annealing model was proposed, as schematically shown in Figure 2.10(c). During the hydrogen plasma treatment, many hydrogen atoms permeate into the sub-surface (growth zone), resulting in the crystallization of an amorphous network through the formation of a flexible network with a sufficient amount of atomic hydrogen in the sub-surface region without remarkable removal process of Si atoms (Nakamura *et al*., 1995; Matsuda, 1999).

These three models have been carefully examined, and the merits and demerits for each model have been discussed (Matsuda, 1999; Saito *et al*., 1998). Apart from that, more microscopic and progressive observations have been reported using in situ diagnostic techniques, and a detailed mechanism underlying the formation process of nc-Si:H has been proposed.

The external energy provided by the ion bombardment has improved crystallinity in the low temperature epitaxial using sputtering, which has been reported to be due to a low energy ion flux (Shindoh and Ohmi, 1996). In contrast, the disrupting role of ions also has been reported (Kondo *et al*., 2000; Matsuda *et al*, 1983; Konuma *et al.*, 1987) in the PECVD processes from the substrate bias effect on the crystallinity. The positive ions in the plasma are accelerated in the sheath region, as shown in Figure 2.1. For the conventional rf PECVD, the energy of the plasma potential is able to break the Si-Si network. Furthermore, the film structure is sensitive to the presence of impurities, such as oxygen and carbon, which can influence the crystal growth. When using the UHV system, an enlargement of the grain size in the temperature range above 350°C is noted (Kamei *et al.*, 1998), while in this temperature regime, the impurity effect on the crystal growth is observed, due to the complete surface coverage.

The nucleation of crystallites does not occur directly on the foreign substrate. As shown in Figure 2.11 (Fujiwara *et al*., 2001), the crystal growth starts to occur after the formation of an amorphous incubation layer. The incubation thickness decreases with the hydrogen dilution ratio. The incubation layer is amorphous, but has a different structure compared to "normal" amorphous silicon, i.e. (1) higher compressive stress and (2) the presence of Si-H complex in the near surface region. The compressive stress appears as a higher frequency shift of the Raman spectrum. The usual amorphous silicon shows a TO phonon peak centered around 480 cm^{-1}, while the incubation layer shows a peak centered around 485-490 cm^{-1} (Kondo *et al*., 1996; Guha *et al*., 1999).

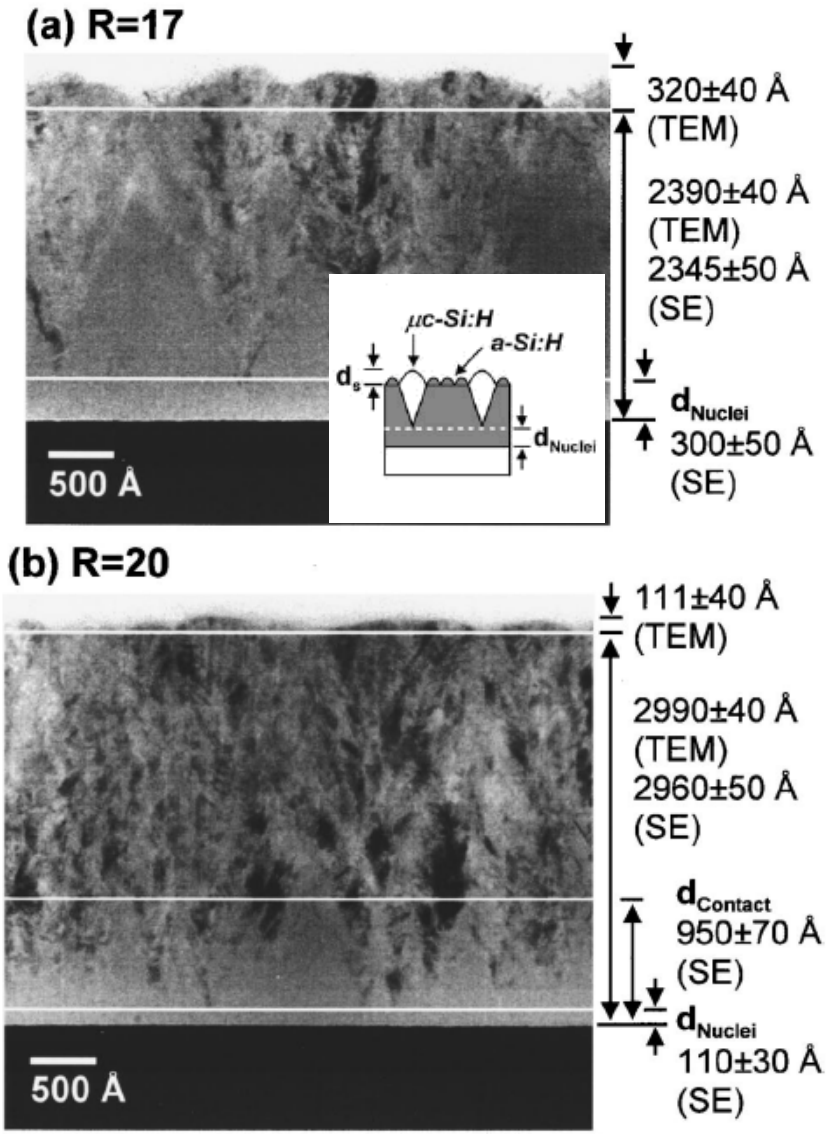

Figure 2.11: Cross-sectional TEM images of the n*c*-Si:H thin films on c-Si substrates. The d_{Nuclei} and $d_{Contact}$ denote the film thicknesses at which the n*c*-Si:H nucleates from the *a*-Si:H phase and the n*c*-Si:H nuclei make contact on the surface, respectively. The thicknesses were determined from the spectroscopic ellipsometry (Fujiwara *et al*., 2001).

The mechanical stress measurement also shows the increasing compressive stress on approaching the nanocrystalline phase boundary by increasing the hydrogen dilution ratio, *R* (Gotoh. *et al*., 1998). The Si-H complex vibration mode is different from the usual Si-H stretching mode either in the bulk (~ 2000 cm^{-1}) or on the surface (~ 2090 cm^{-1}) in the infrared absorption spectrum. This Si-H complex originates from the three center bond, Si-H-Si, and its density increases with increasing hydrogen dilution ratio and growth temperature. Moreover, the nucleation occurs when the density of this complex reaches the critical value (Fujuwara *et al*., 2002).

2.4 Influence of Deposition Parameters in PECVD nc-Si:H Thin Films

2.4.1 Effects of Discharge Power and Hydrogen Dilution on Deposition

The effects of discharge power have been widely studied by (Lin *et al*., 2003), indicating that the discharge power playing a role in dissociating the SiH_4 and H_2 to produce SiH_x (x = 1, 2, 3) radicals and atomic hydrogen in the plasma of PECVD. This mean high discharge power is more effective in promoting the dissociation of the radicals and the atomic hydrogen. A high density of the growth precursors, SiH_3, has been reported to enhance the growth rate; however, the incidence of disorders or defects increases at high deposition pressure (Cabarrocas *et al*., 2002). Besides, an increase in discharge power promotes more atomic hydrogen reaching the growth surface, therefore enhancing the hydrogen etching effect. As a result, the nucleation sites are enhanced, thus increasing the crystalline volume fraction of the film. High rf power has also been reported to produce larger crystallite size of nc-Si:H (Das, C. and Ray, S., 2002; Fujiwara *et al*., 2001). In addition, the crystalline volume fraction and deposition rate of the film decreases with a further increase in discharge power due to excessive ion bombardment on the growing surface and promotes the growth of the amorphous phase (Kondo *et al*., 2000).

Figure 2.12 shows a phase diagram depending on a wide variety of deposition parameters (Matsuda, 1999). In the low discharge power regime, where the ion bombardment is small, the crystalline phase appears in the high hydrogen dilution regime. This transition occurs sharply with increasing hydrogen dilution ratio, *R* (Li *et al.*, 2010; Guo *et al.,* 2011). In the low dilution ratio regime, contrastingly, the structure is amorphous for the low discharge power, the crystalline phase appears in the high discharge power region and finally the amorphous phase appears again in the highest power region. The formation of microcrystalline silicon under high density plasma with pure silane, without hydrogen dilution, has also been reported (Scheib *et al*., 1996; Shirai *et al*., 1999).

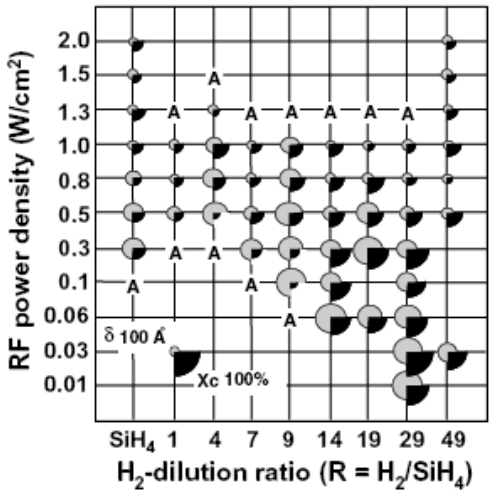

Figure 2.12: Crystal size (three quarter gray circles: *d*) and volume % (quarter solid circles: X_C) of microcrystallites in the resulting films mapped out on the RF power density/hydrogen dilution ratio plane (Matsuda, 1999).

2.4.2 Effects of Substrate Temperature

The substrate temperature, T_s is one of the important parameters, which control the surface reactions in the growth kinetics (Das *et al*., 2004; Mukhopadhyay, *et al*., 2001). Meanwhile, the crystalline volume fraction increases with the increase in

substrate temperature. The network structure of a thin film is determined by the energy relaxation of the adatoms on the growing surface. A compact and well-defined structure is obtained if the precursors have a large diffusion coefficient. At a high hydrogen dilution and for T_s of 350°C, the film growing surface is considered to be totally covered with atomic hydrogen.

The SiH_3 radical is the main film growing precursor, and it has the longest reaction lifetime among all SiH_x (x = 0–3) radicals generated in plasma. These SiH_3 radicals are absorbed on the H-covered growing surface. A fraction of them diffuse and reach the stable sites for nuclei formation by the following chemical reactions: ≡SiH + SiH_3 → ≡Si +SiH_4 and ≡Si + SiH_3 → Si–SiH_3, where ≡Si represents a dangling bond of Si. The remaining precursors are desorbed, depending on their sticking coefficient on the surface. So, at a high H_2 dilution, the Si:H films have a nanocrystalline nature, even though they are deposited at a low substrate temperature.

Figure 2.13 shows the crystalline volume fraction in the resulting nc-Si:H as a function of substrate temperature during the film growth for three different hydrogen to silane flow-rate ratios (Matsuda, 1999). The deterioration in the crystallinity can be seen in the high temperature regime, T > 400°C, where the surface hydrogen starts to become thermally desorbed. The absence of nc-Si formation above 500°C indicates that the surface hydrogen coverage is one of the important conditions for the crystallites formation in the resulting film (Matsuda, 1983). However, with a high atomic hydrogen density in the chemical transport experiment, the thermal evolution of surface hydrogen can be recovered and a sufficient amount of surface coverage can be maintained, even at high temperature. Similar high temperature behaviour is observed in the epitaxial growth (Kitagawa *et al*., 2000).

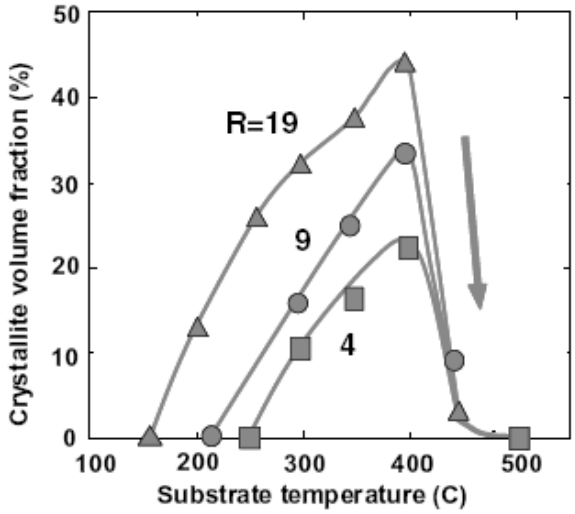

Figure 2.13: Volume % (X_C) of microcrystallites in the resulting films plotted against the substrate temperature during film growth for three R_s (Matsuda, 1999).

2.5 High Rate Growth of Nanocrystalline Silicon

It appears that the low temperature growth requires a critical balance in the formation of nanocrystalline structure from amorphous structure (Veprek and Marecek, 1968). In fact, the low temperature nanocrystalline growth has the maximum growth rate, as limited by the growth temperature (Jorke *et al.*, 1989). However, a high growth rate in mass production is crucial, and a growth rate above 50 $Å s^{-1}$ is required, assuming the thickness to be more than 2 μm. The growth rate is determined by the flux density of the film precursors, such as the SiH_x radicals, and the generation rate of radicals, G_r is given by the following expression,

$$G_r = n_e \upsilon_e N_g \sigma_d , \tag{2.2}$$

where n_c and υ_e are the density and velocity of energetic electrons, respectively, with a kinetic energy higher than the dissociation threshold of the source gas molecule, such as SiH_4. N_g and σ_d are the density and the dissociation cross section of the source gas molecule, respectively.

A novel method, termed the high pressure depletion (HPD) method (Kondo *et al.*, 2000; Fukawa *et al.*, 2001), combines the high pressure and high RF power for a high growth rate of high quality nanocrystalline silicon. The high gaseous pressure increases the gas density N_g and reduces the ion bombardment, while it decreases the atomic hydrogen density due to the recombination. The high rf power increases the electron density and suppresses the hydrogen annihilation reaction, while it increases the ion bombardment. The combination of the two conditions enhances both their advantages and compensates for the drawbacks with each other. As a result, a growth rate of 15 $Å s^{-1}$ can be realized, and these values are reasonable for the application method (Guo *et al.*, 1998). Further development has been achieved using VHF plasma, and device grade films with a defect density of 2.6×10^{16} cm^{-3} have been obtained at 58 $Å s^{-1}$ (Kondo *et al.*, 2000; Fukawa *et al.*, 2001). A similar high growth rate using UHF plasma has been reported (Shirai *et al.*, 1999). The suppression of the ion damage at high gaseous pressure is beneficial for reducing the extent of defects.

Non-plasma processes have also been extensively studied for nanocrystalline silicon fabrication. The hot-wire method (or catalytic CVD) method utilizes the catalytic pyrolysis of source gas molecules on the heated surface of a specific metal, such as tungsten (Matsumura, 1998). The advantage of the catalytic process is the efficient dissociation of hydrogen as well as silane. The fundamental mechanism of this process has recently made significant progress (Tange *et al.*, 2001; Nozaki *et al.*, 2001), and material properties and solar cell performance have been improved (Mahan, 2001; Schroder *et al.*, 2001) for not only a-Si:H but also nanocrystalline silicon solar cells.

2.6 Structural Properties of Nanocrystalline Silicon

The nanocrystalline silicon consists of small crystallites of the order of 10 nm embedded within an amorphous matrix. A crystallite > 10 nm shows a nearly identical

spectrum to the single crystalline silicon, centered at 520.5 cm^{-1}, and its width mainly depends on the internal stress distribution. Amorphous silicon shows a broad and nearly symmetric lineshape centered at ~ 480 cm^{-1} in the Raman spectrum. A simple calculation based on the phonon dispersion relation and its size effect indicates the asymmetric lineshape and the low frequency shift of the peak position of the Raman spectrum for small crystallites < 10 nm, as shown in Figure 2.14 (Campbell and Fauchet, 1986; Kanemitsu *et al.*, 1993).

It should be noted that a peak shift also occurs due to the mechanical stress in the film. For single crystalline silicon, the Raman shift due to stress has been extensively studied by Cerdeira *et al.*, 1972. The volume fraction, X_C of the crystalline phase in microcrystalline silicon is estimated by the following equation,

$$X_c = I_c \Big/ \left(I_c + \gamma I_a\right), \tag{2.3}$$

where the I_c, I_a and γ are integrated intensity of amorphous and crystalline components and scattering efficiency ratio, respectively. The value of γ has been estimated at 0.88 (Tsu *et al.*, 1982). Here, the contribution of the crystallites is usually smaller than several nm and difficult to evaluate because the scattering efficiency is unknown.

The XRD measurements provide information on the lattice constant, crystallite size and orientation. The lattice constant has deviated from that of single crystalline silicon due to strain and the strain can be compared to the Raman peak shift. For instance, isotropic compressive stress induces a higher frequency shift in the Raman peak and reduced lattice constant, while the biaxial strain due to such a thermal (compressive) stress results in a higher frequency shift in the Raman peak and the expansion in the lattice constant, because the XRD usually measures the lattice constant normal to the substrate.

The randomly orientated nanocrystalline silicon shows peak intensity ratios 1:0:0.55:0.3 among (111), (222) and (311) diffraction peaks respectively, whereas a

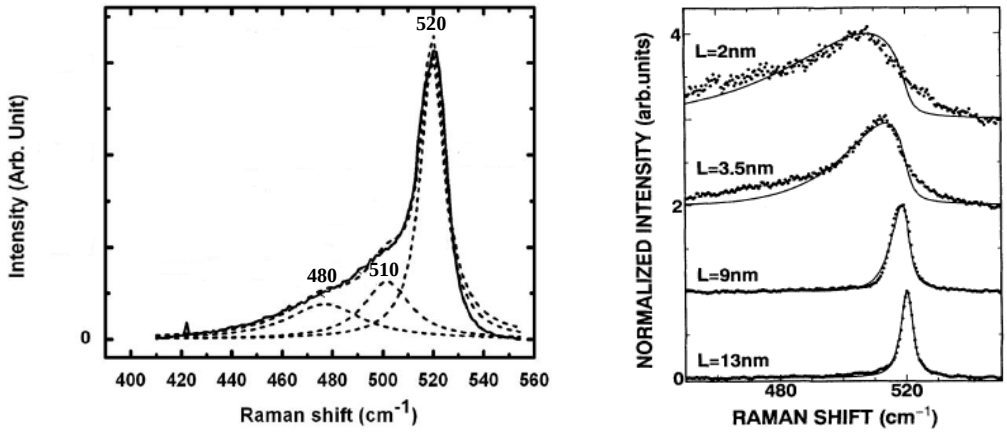

Figure 2.14: Size dependence of Raman spectra (right, the vertical axis gives the signal intensity in arbitrary units) for size-controlled nanocrystalline silicon and a typical Raman spectrum (left) of mixed phase sample prepared by PECVD. The dotted line in the left figure designates the amorphous, nanocrystalline (~ a few nm) and large crystallite (> 10 nm), components obtained from simulation (Kanemitsu *et al.*, 1993).

preferential orientation is found under various deposition conditions (Kiriluk *et al.*, 2011). The most commonly observed preference is the (220) orientation as shown in Figure 2.15. The cross sectional transition electron micrograph (XTEM) shows a columnar structure in the film with the (220) preferential orientation. Other preferential orientations along (400) directions have been reported (Kamiya *et al.*, 1999). A difference in the etching rates among different orientations of crystallites may play an important role.

The grain size is commonly evaluated using Sherrer's formula. Strictly speaking, however, in the case of the anisotropic shape of the crystallite, as shown in Figure 2.15, this estimation can lead to a significant error. In fact, the TEM observation reveals the columnar shape with a diameter of about 20 nm and a longitudinal axis of 1 μm.

Nanocrystalline silicon prepared at low temperatures contains a lot of hydrogen in the film, at a typical density of around 3-5 at %. The hydrogen amount is rather lower than that of a-Si:H (10 at % typically) (Brodsky *et al.*, 1977), and the hydrogen is thought to precipitate on the surface of the grain boundaries. A simple calculation,

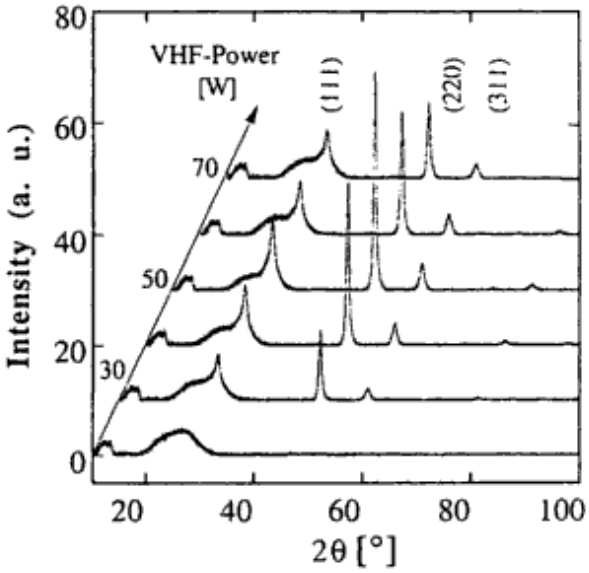

Figure 2.15: XRD patterns for nanocrystalline silicon prepared at different rf powers.

where columns with a diameter of 20 nm are packed closely, indicates the number of surface dangling bonds of the order of 1 at % of silicon, which is consistent with the observed amount of incorporated hydrogen. Figure 2.16 shows typical IR absorption spectrum of highly crystallized nanocrystalline silicon, together with that of a-Si:H for comparison. The device grade a-Si:H shows a typical absorption peaks at 2000 and 630 cm^{-1}, while nanocrystalline silicon shows peaks at 2100 cm^{-1}, and this is attributed to the surface Si-H mode on the grain boundaries and/or the SiH_2 mode, because the SiH_2 wagging and bending mode (845 and 490 cm^{-1}) are also observed. Poor crystallinity samples show both 2100 and 2000 cm^{-1} components. Since the μc-Si contains a high density of grain boundaries with a columnar structure, the grain boundaries tend to be oxidized during the air exposure. The post-oxidation affects the electrical conductivity as well as the defect density (Kondo *et al.*, 1998; Goerlitzer *et al.*, 1998).

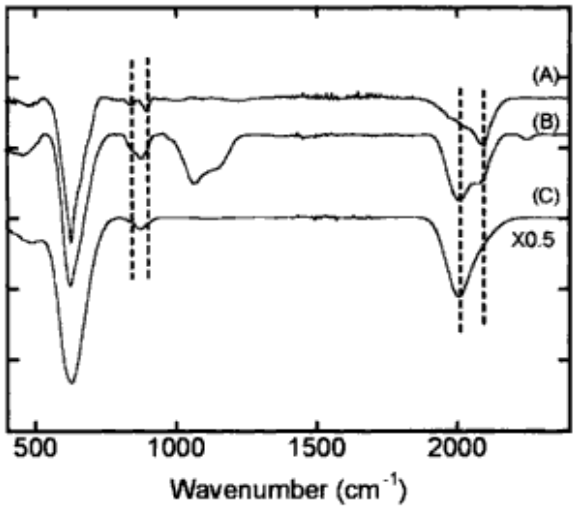

Figure 2.16: FTIR spectra for highly crystallized sample (I_c/I_a = 8.5, *A*), moderately crystallized sample (I_c/I_a = 4.3, *B*) and a-Si:H prepared at high growth rate (*C*). The four dashed lines designate 845, 890, 2000 and 2100 cm^{-1}, respectively. Sample (*B*) shows the absorption peak around 1000 cm^{-1} due to the post oxidation (the vertical axis gives the absorbance in arbitrary units).

2.7 Optical Properties of Nanocrystalline Silicon

The optical properties of nc-Si:H are of great importance in order to understand the interaction of incident photons with the material, which are divided into optical absorption and emission. The optical absorption characteristics are usually described by optical transmission spectroscopy in order to obtain the absorption coefficient, the refractive index and the optical band gap. The optical emission feature is characterized by photoluminescence spectroscopy.

2.7.1 Optical Absorption Spectroscopy

The optical absorption spectrum is one of the most important physical quantities reflecting the nature of hydrogenated nanocrystalline silicon (nc-Si:H), which is quite similar to a-Si:H, and most of the optical models have been applied to nc-Si:H in order to explain the optical characteristics of the material. The optical absorption spectrum

can be observed by the band to band transition, i.e., the electronic excitation from the valence band into the conduction band. The threshold at the low energy side of the optical absorption spectrum is called optical absorption edge and corresponds to a separation in energy between the bottom of the conduction band and the top of the valence band (Morigaki, 1999). As shown in Figure 2.17, the absorption edge spectrum of amorphous semiconductors can be roughly divided into three regions (Tauc, 1974): the high absorption region *A* (optical absorption coefficient: $\alpha>10^3 cm^{-1}$), the exponential edge *B* ($10^1<\alpha<10^3 cm^{-1}$) and the weak absorption tail *C* ($\alpha<10^1 cm^{-1}$). The optical transitions in response to each region are shown in the simplified gap-state profile of Figure 2.18 (Tanaka, 1989). This scheme assumes the optical ***k*** selection rule is completely relaxed on the basis of the random phase approximation for wave function (Hindley, 1970; Mott and Davies, 1979), which means the optical absorption spectrum is expressed as a convolution of the density of states,

$$\alpha(hv) \mu \int_{E_F - hv}^{E_F} N(E)N(E + hv)dE/hv, \tag{2.4}$$

where E_F is the Fermi energy, *hv* the photon energy, and N(*E*) the density of states at an energy *E* (Yamasaki *et al.*, 1982; Tanaka and Yamasaki, 1982).

The optical transition of region *A* corresponds to the electron excitation from the valence band to the conduction band. This region is usually described as the Tauc expression:

$$(\alpha E)^{1/2} = B(E - E_G), \tag{2.5}$$

where *B* is the constant containing an average matrix element and E_G is the constant energy, which is defined as the optical band gap energy between the conduction and valence band-edges in nc-Si:H (Cavalcoli *et al.*, 2011).

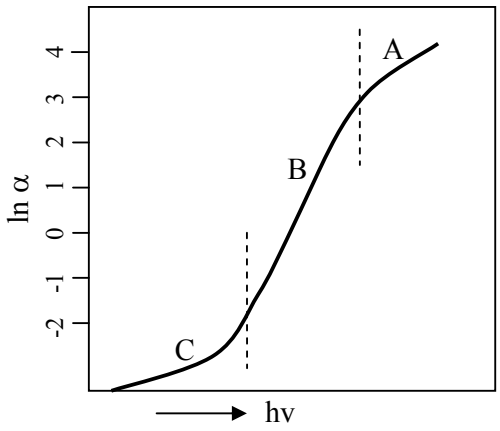

Figure 2.17: Part A, B and C of the optical absorption edge of amorphous semiconductors (Tauc, 1974).

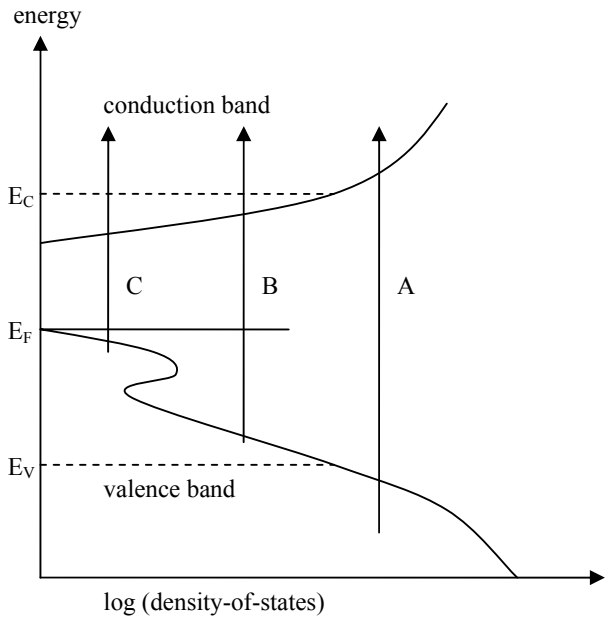

Figure 2.18: Simplified profile of density of state as a function of energy in amorphous semiconductors. E_c, E_v, and E_F are conduction and valence band edges, and Fermi level, respectively. Optical transition *A*, *B* and *C* correspond to those of Figure 2.17, respectively (Tanaka, 1989).

The *B* region, roughly in the range of $10^1 cm^{-1} < \alpha < 10^3 cm^{-1}$, shows an exponential variation of α with hv;

$$\alpha = \alpha_o \exp\left(\frac{hv}{E_e}\right), \tag{2.6}$$

where α_o is the constant and E_e the characteristic energy representing the slope of the exponential tail. This region has been attributed to an exponential tail of the valence or conduction band, and reflects the randomness of an amorphous network (Yamasaki, 1987; Cody *et al*., 1981). The weak absorption tail of region *C* is attributed to the deep states in the mid-gap, mostly originating from defects and impurities. The optical absorption range below the optical band gap (i.e. regions *B* and *C*) includes important information for the understanding of a-Si:H and varies with the thermal history, impurities and preparation conditions.

2.7.2 Photoluminescence emission spectroscopy

Photoluminescence (PL) emission spectroscopy is a technique which is widely used to study the recombination processes and electronic properties of a-Si:H. The large density of the localized tail states, especially of the valence band tail states, is the major influential factor in the PL processes in a-Si:H. Figure 2.19 shows the schematic diagram of the PL processes that comprise photon-excitation of electron-hole pairs, carrier thermalization and recombination. The recombination occurs after the carriers are trapped into the band tail states. There are two competing recombination channels, i.e. the radiative and non-radiative recombination. The former involves the conversion of excitation energy into photons, the latter the conversion of the excitation energy into phonons. PL is a measure of the photon emission via radiative recombination. The dominant recombination mechanism between band tail states is radiative transition and the dominant recombination mechanism from band edge to defect states is non-radiative transition.

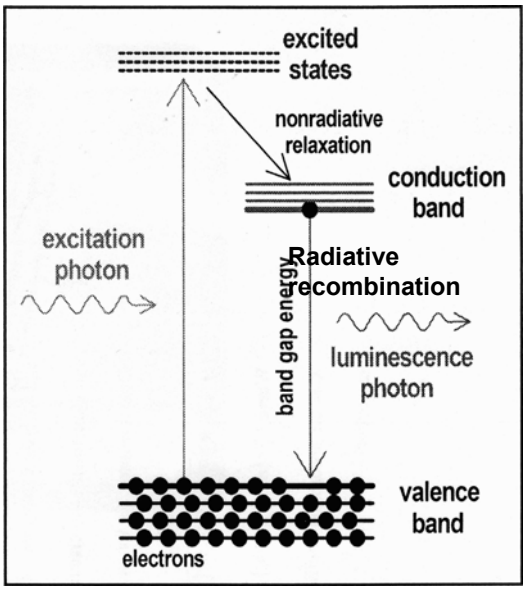

Figure 2.19: Schematic diagram of the PL processes in a-Si:H.

The recent trend in the development of semiconductors usable as optical devices is to prepare quasi-direct-gap semiconductors as nanocrystalline silicon (nc-Si), which exhibit strong visible photoluminescence spectra, even at room temperature (RT). This phenomenon of PL emission was explained by the quantum confinement effect (QCE), entailing a widening of the band gap of the material due to the presence of nanocrystallites embedded within an amorphous matrix. Veprek *et al.* prepared nc-Si:H films by hydrogen diluted silane plasma or by chemical transport of silicon in hydrogen plasma (Veprek *et al.*, 1995). However, similarly to porous silicon (PS) (Canham, 1990; Lehmann and Foll, 1990), these films exhibit a PL improvement only after post annealing or oxidation. The deposition of nc-Si films utilizing hydrogen diluted silane, commonly employed for the production of microcrystalline or polycrystallline silicon, has also been reported by Liu *et al.*, 1994. They reported the production of nc-Si grown at temperatures lower than 200°C and exhibiting RT visible PL at 1.82 eV.

The PL intensity and the PL spectrum are sensitive to the surface chemistry of nc-Si, particularly with regard to the amounts of oxygen and hydrogen on the surface

(Kanemitsu *et al.*, 1997; Chin *et al.*, 1995). The PL peak energy in H-terminated nc-Si is very sensitive to the nanocrystal size, compared with surface-oxidized nc-Si (Kanemitsu and Okamoto, 1997). Figure 2.20 shows PL spectra of Si nanocrystals embedded in SiO_2 prepared by co-sputtering of Si and SiO_2, and annealing at temperatures higher than 1100°C (Takeoka *et al.*, 2000). By controlling the size, the luminescence maximum shifts from close to the bulk Si band gap to 1.6 eV. The luminescence properties of H-terminated nc-Si are considered to be different from those of surface-oxidized nc-Si. Recently, Shim *et al.*, 2004 found that the PL peak position gradually shifts from 2.58 eV to around 1.77 eV, as the H_2 flow rate increases from 50 to 100 sccm. They suggested that the PL peak position shifts due to the increase in the grain size from around 2 nm to around 8 nm. In addition, they studied the effect of annealing temperature on PL property and found a change in the intensity as well as the peak position, which is caused by the change in the total volume and the grain size in the films, respectively. The effects of surface passivation of nc-Si of different sizes with hydrogen or oxygen at different temperatures on the observed PL were investigated by Dinh *et al*., 1996. This nc-Si showed strong infrared and/or visible PL when passivated by hydrogen or oxygen.

Although there have been numerous research studies in recent years, the mechanism underlying the visible luminescence is still unclear (Kanemitsu, 1995; Cullis *et al.*, 1997; Wu *et al.*, 2003). So far, two main models have been proposed for the interpretation of the origin of the visible PL. The first one is the QCE model (Cullis and Canham, 1991) and the second is the surface state model (Koch *et al*., 1992). As known, two major mechanisms of PL processes are the formation of photoexcited carriers (excitation process) and the radiative recombination of the photoexcited carriers through PL centers (luminescence process). For the QCE model, it is considered that both the excitation process and the PL process originate from nc-Si. For the surface

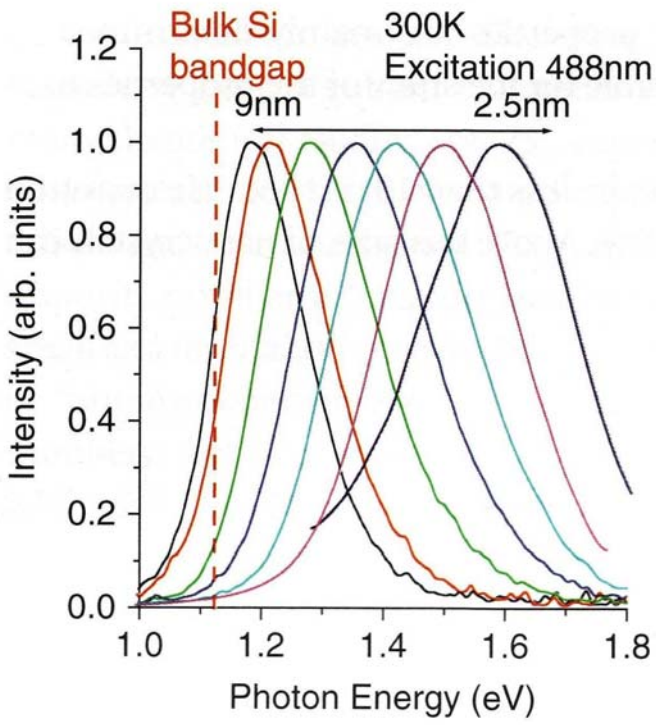

Figure 2.20: PL spectra of Si nanocrystals embedded in SiO_2 thin films at room temperature. The average diameters are changed from about 9 to 2.5 nm (Takeoka *et al.*, 2000).

state model, it is considered that the excitation process originates from nc-Si and the PL process originates from a special surface state. As for the surface state model, various surface species, such as siloxene, polysilanes, SiH_2, Si band-tail states and interfacial oxide-related defect centers have been suggested as the source of the visible PL (Ali, 2007).

The fabrication of nc-Si:H films, having a highly efficient QCE, requires both a reduction in the grain size, d and an enhancement in the crystalline volume fraction, X_C. In that case, an increase in the nucleation rate would become a key technique to be developed. It has been reported that the enhanced nucleation on the growing surface during deposition of nc-Si can be achieved by increasing the hydrogen flow rate, R (Milovzorov *et al.*, 1998; Kim *et al.*, 1995) or the deposition temperature, T_d (Lim *et al.*, 1996). However, the increase in T_d also caused an increase in d. Thus, the increase in R

leads to the reduction of d, while the increase in T_d should lead to an increase in d. Furthermore, it has been reported that the formation of nc-Si is also due to the higher etching activity of hydrogen radicals for the amorphous phase than the crystalline one (Solomon *et al.*, 1993; Oda and Odobe, 1995).